

Evaluation of the GPS Positioning Error due to the Inhomogeneous Distribution of Atmospheric Delay by a Numerical Weather Model Data

Hironmu Seko

(Meteorological Research Institute/JMA)

Hajime Nakamura

(Numerical Prediction Department / JMA)

Sei-ichi Shimada

(National Research Institute for Earth Science and Disaster Prevention)

-Contents-

1. Motivation

2. Methodology

**3. Positioning error caused by Mountain lee wave
Comparison with observed results (Shimada, 2002)**

4. Summary

1. Motivation

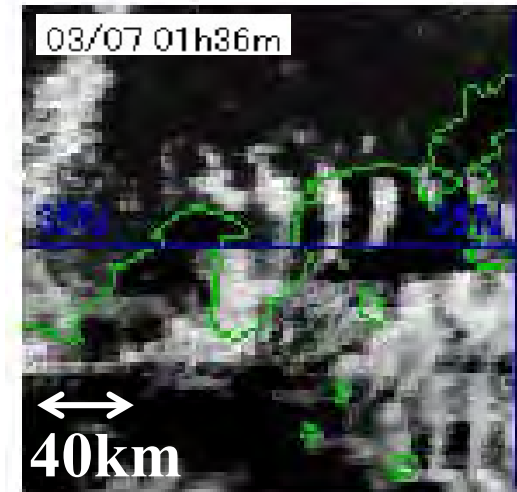
- Large positioning errors were caused by atmosphere.
- Atmospheric model with gradient does not always improve positioning error.

→ **Small scale variation existed?**

- To discuss only influence of atmosphere, **'clean' delay was calculated by the numerical weather model.**

- 'Clean' delay was used as input data of analysis program and positioning error was estimated.

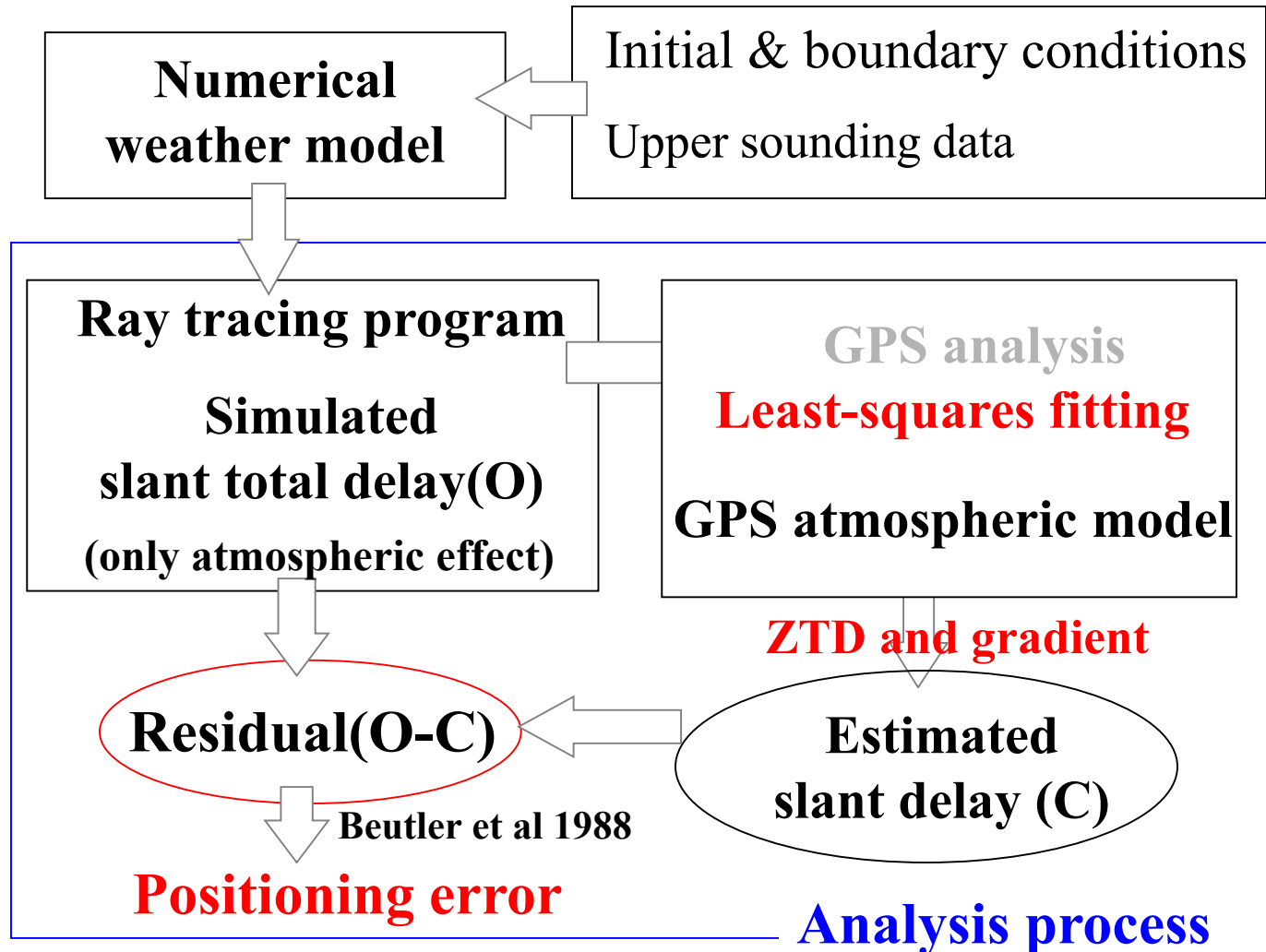
- **Small scale variation (mountain lee wave case) causes the positioning error?**



Cloud images observed by geostationary meteorological satellite

2. Method

2.a Flowchart of estimation of positioning error



2.b Atmospheric model

(a) Constant model

$$\tau_{\text{est}} = \tau_{\text{zen}} m(\theta)$$

(b) Linear gradient model (MacMilan, 1995)

$$\tau_{\text{est}} = \tau_{\text{zen}} m(\theta) + m(\theta) / \tan(\theta) (G_N \cos\phi + G_E \sin\phi).$$

(c) Second order function fitting model

$$\tau_{\text{est}} = \tau_{\text{zen}} m(\theta) + m(\theta) (G_N y + G_E x + G_{N2} y^2 + G_{NE} xy + G_{E2} x^2),$$

where $x = 1.0 / \tan(\theta) * \sin\phi$, $y = 1.0 / \tan(\theta) * \cos\phi$

2.c Estimation of positioning error

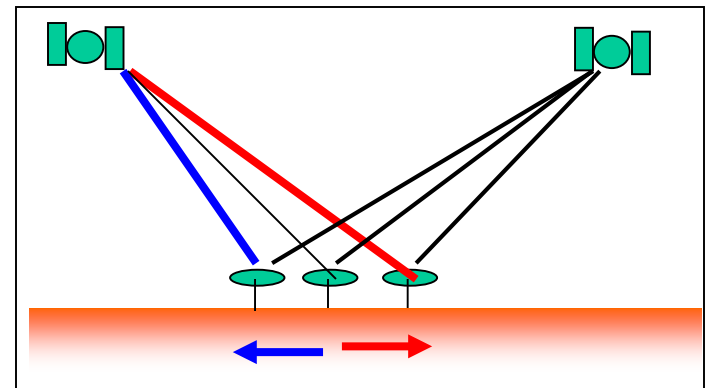
When estimated slant delay (τ_{est}) is **larger** (**smaller**) than simulated delay (τ), the receiver position was shifted to **opposite** (**same**) side of satellite.

Positioning error (Beutler, 1988):

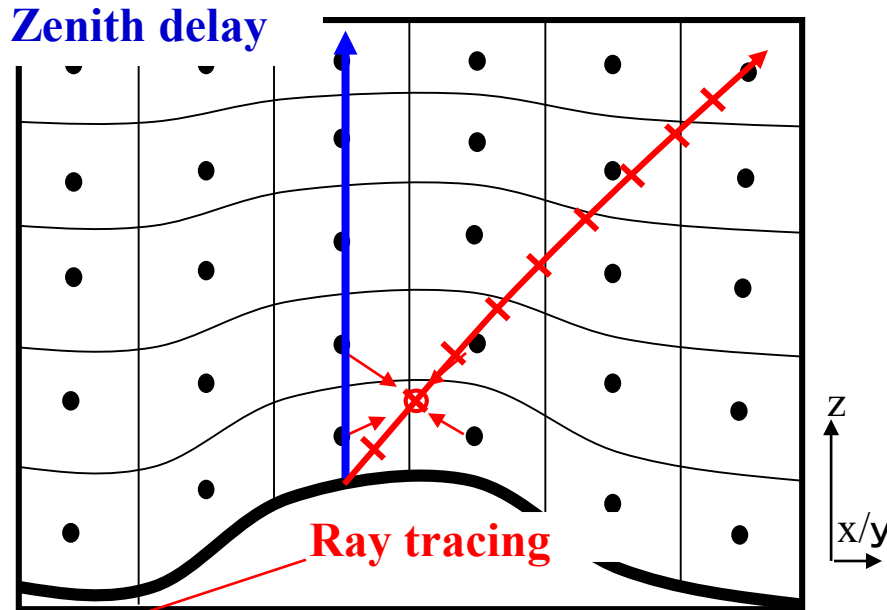
$$\delta x = -\sum \{(\tau - \tau_{\text{est}}) \cos\theta \sin\phi\} / N,$$

$$\delta y = -\sum \{(\tau - \tau_{\text{est}}) \cos\theta \cos\phi\} / N,$$

$$\delta z = -\sum \{(\tau - \tau_{\text{est}}) \sin\theta\} / N$$



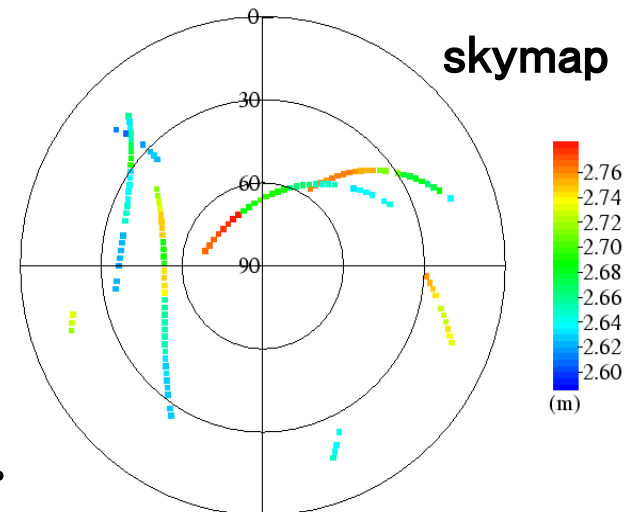
Analysis process



Numerical weather model

- Non-hydrostatic model of Meteorological Research Institute
- Variables: U V ρ P θ
 q_v q_c q_r q_s q_h q_i etc.
- Horizontal grid : 250m
- Initial data: upper sounding

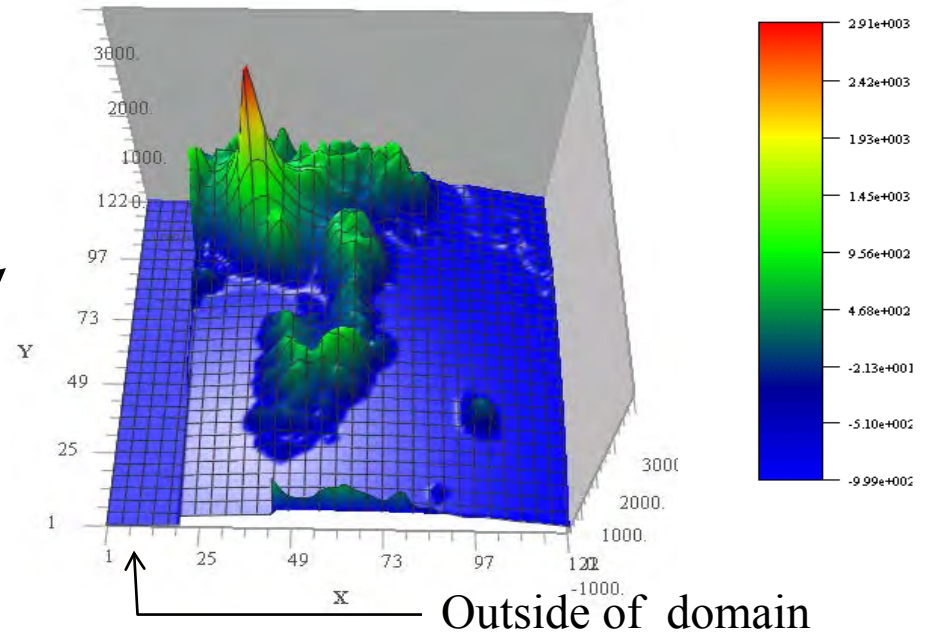
1. **Actual positions** of GPS receivers and satellites were used. (cutoff angle 15°)
2. The path was found by using the **ray tracing method**.
3. Slant delays were obtained by integrating the delay along the path.



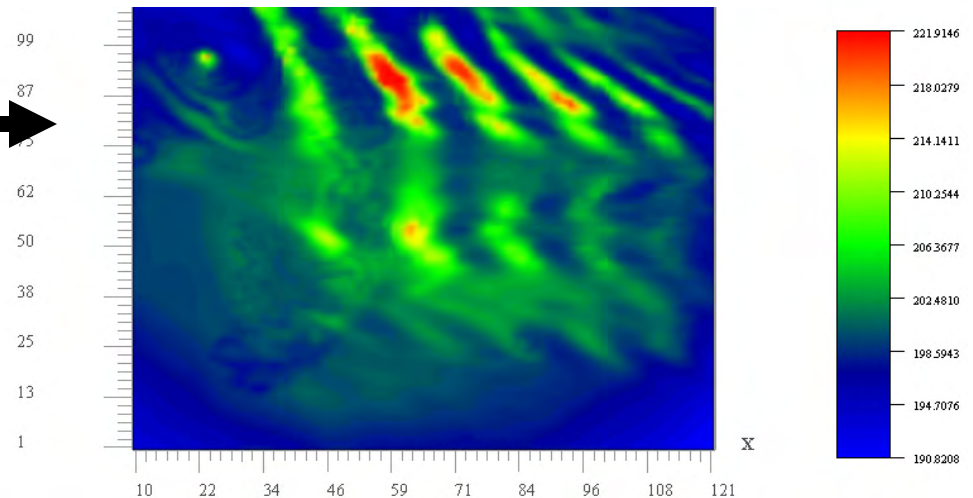
Cartesian grid relative to a receiver

- **Curvature of the earth** was taken into account.
- **NHM model**
Latitude, Longitude, Height
→ Cartesian orthogonal coordinate relative to a receiver opposition
 $\Delta x, \Delta y = 250\text{m}, \Delta z = 100\text{m}$
- **Refractivity (N)** on the Cartesian grid was calculated from simulated data (Thayer, 1974).
- **Delay** was calculated from refractivity (N).

Topography relative to GPS receiver



Horizontal distribution of N at z=3km



Outline of ray tracing method

Derivation of equation⁽¹⁾

- $d/ds(n d\mathbf{X}/ds) = \nabla n \dots(1)$
where, \mathbf{X} : position of tracer, n : refractivity, s : increment of tracing distance (100m)
- When $\mathbf{Y} = n d\mathbf{X}/ds$ is introduced, a equation (1) become
 $d\mathbf{Y}/ds = \nabla n \dots(2) \quad d\mathbf{X}/ds = \mathbf{Y}/n \dots(3)$
- Furthermore, $d\tau = ds/n$ is introduced. Equation (2) and (3) became
 $d\mathbf{Y}/d\tau = n\nabla n \dots(2)'$ $d\mathbf{X}/d\tau = \mathbf{Y} \dots(3)'$

Ray tracing technique⁽²⁾

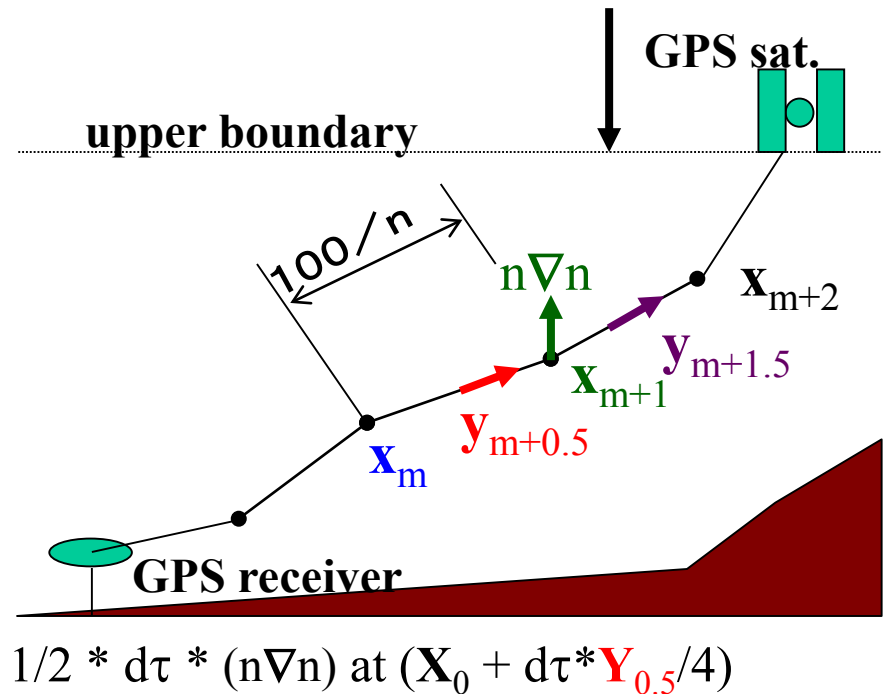
- At the starting point of tracing,
 $\mathbf{X}_0=0, \mathbf{Y}_0 = n_0 d\mathbf{X}/ds$
- \mathbf{X} is calculated as follows;
 $\mathbf{X}_{m+1} = \mathbf{X}_m + d\tau * \mathbf{Y}_{m+0.5}$
 $\mathbf{Y}_{m+1.5} = \mathbf{Y}_{m+0.5} + d\tau * (n\nabla n) \text{ at } \mathbf{X}_{m+1}$
- $\mathbf{Y}_{0.5}$ is estimated, implicitly.
 $\mathbf{X}_1 = \mathbf{X}_0 + d\tau * \mathbf{Y}_{0.5}$
 $\mathbf{Y}_{0.5} = \mathbf{Y}_0 + 1/2 * d\tau * (n\nabla n) \text{ at } \mathbf{X}_{0.25} = \mathbf{Y}_0 + 1/2 * d\tau * (n\nabla n) \text{ at } (\mathbf{X}_0 + d\tau * \mathbf{Y}_{0.5}/4)$

Reference:

¹Principles of Optics, I
Born, Max /Wolf, Emil

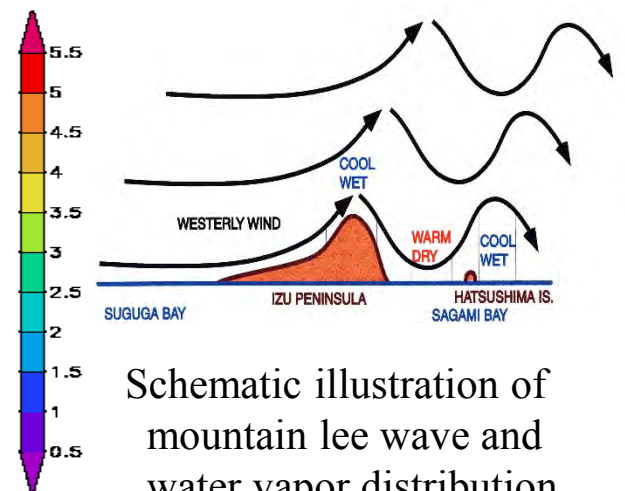
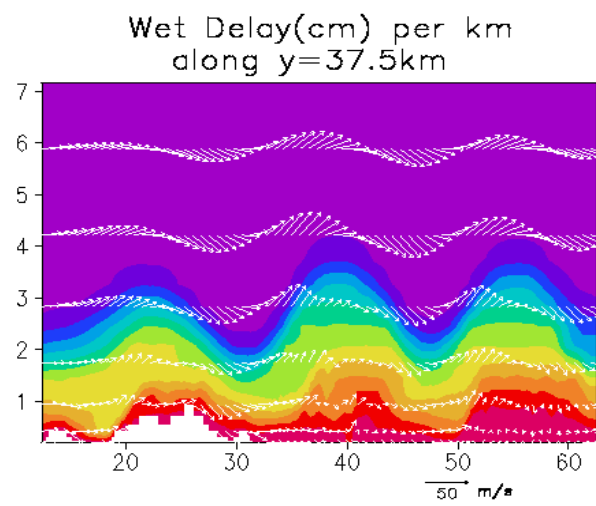
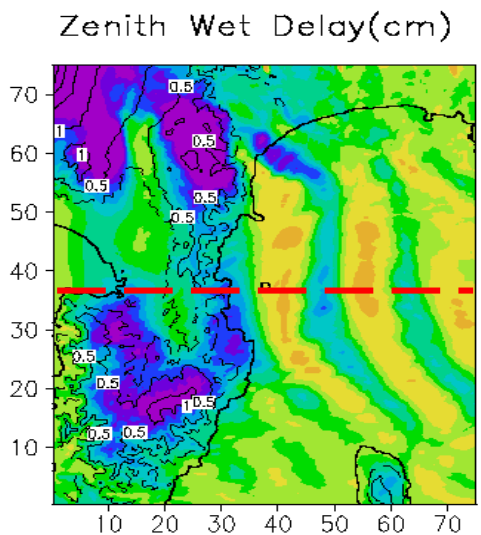
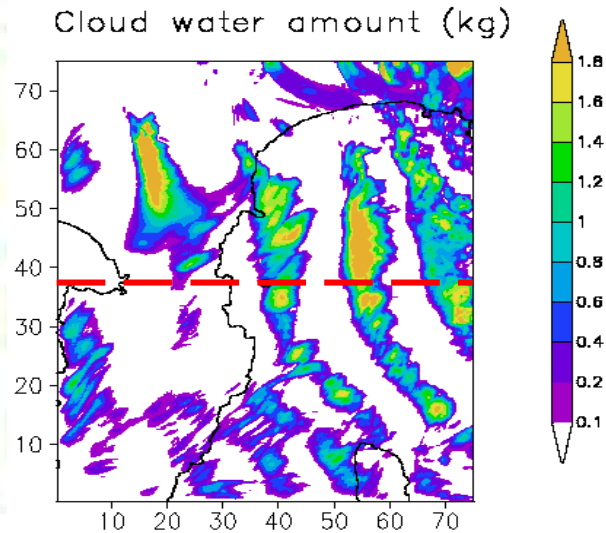
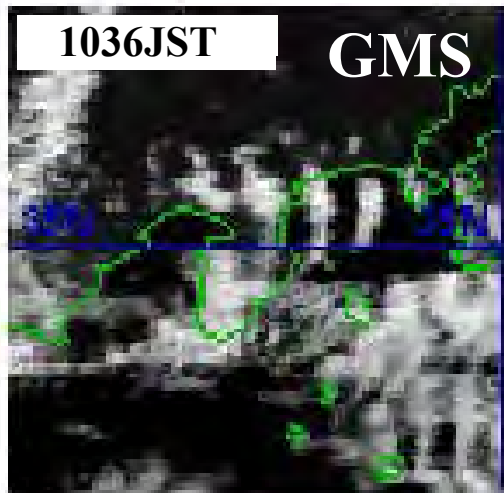
²Direct assimilation of GPS/MET refraction angle measurements, X. Zou *et al.*

Tracers are traced in the three dimensions space. Traces that arrived at the upper boundary of the domain are used.



3. Mountain lee wave simulated by numerical model (7 March 1997)

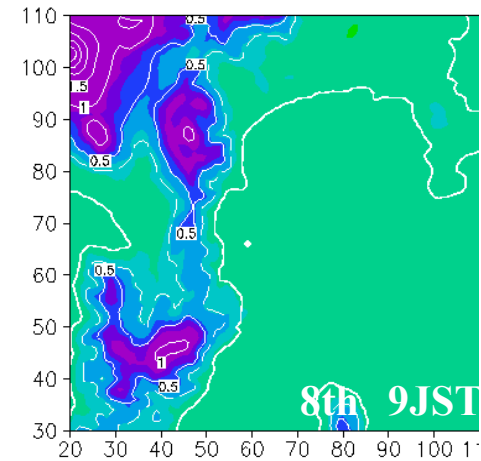
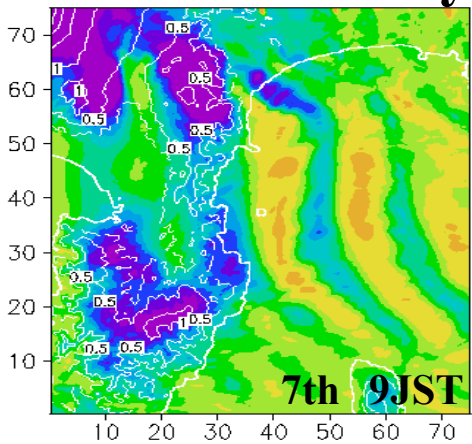
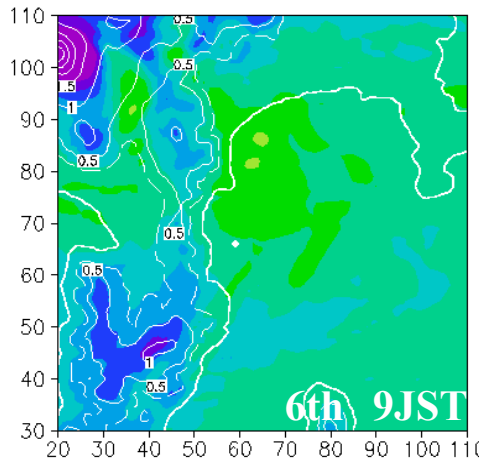
- Line-shaped cloud bands
- Orientation: north-south direction
- Location: East of Izu peninsula
- Wave length: $\sim 15\text{km}$
- Numerical model simulated well mountain lee wave.



Schematic illustration of mountain lee wave and water vapor distribution (Shimada et al. 2001)

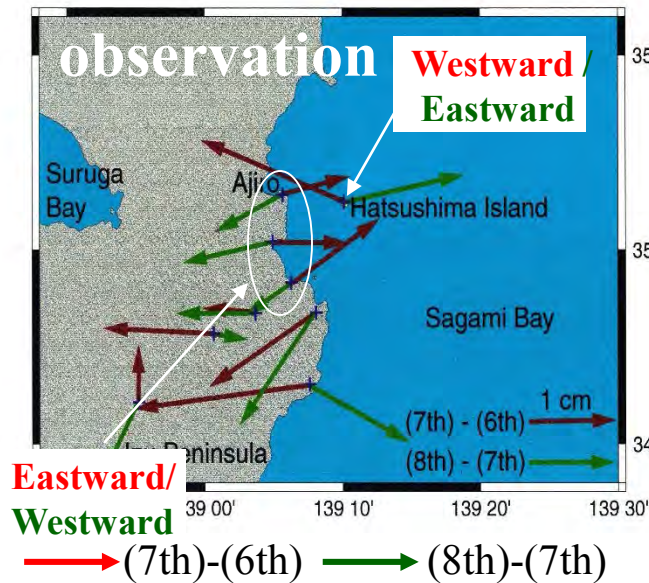
Positions estimated with 'Constant model'

Zenith wet delay

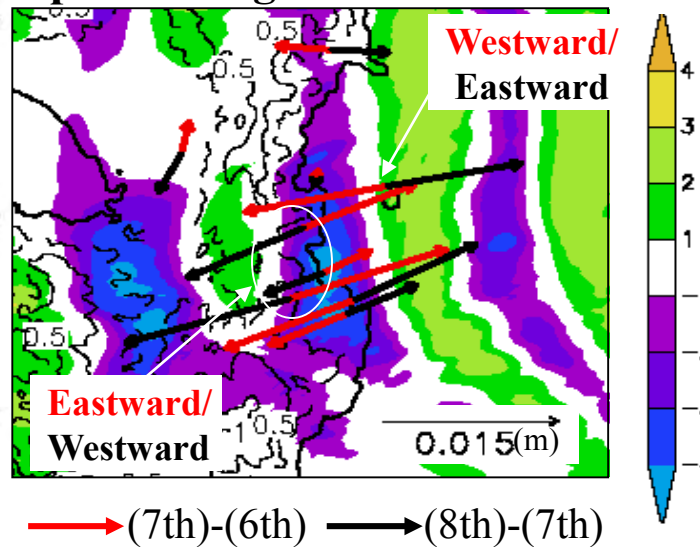


Movement of position with model of $\tau_{est} = \tau_{zen} m(\theta)$.

Positioning error (observation)



Deviation of PWV and positioning error (simulation)

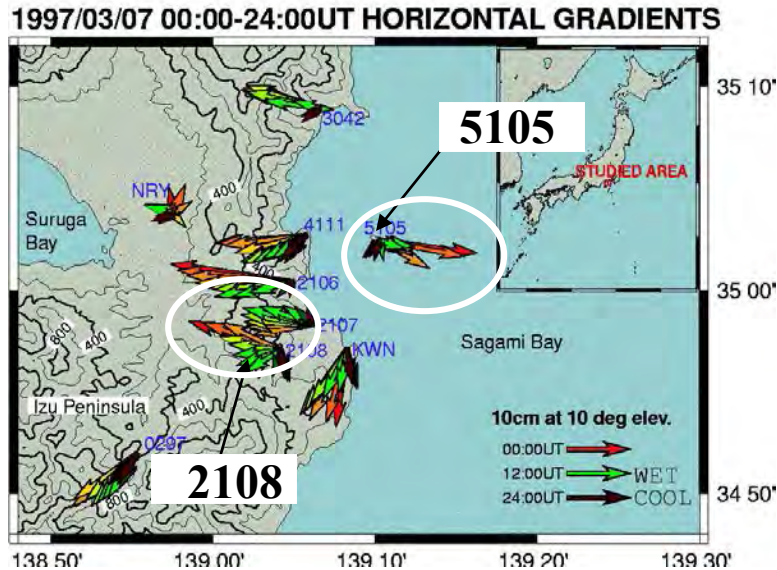


- Numerical model simulated well the feature of positioning error.
- Positioning error was caused by mountain lee wave.

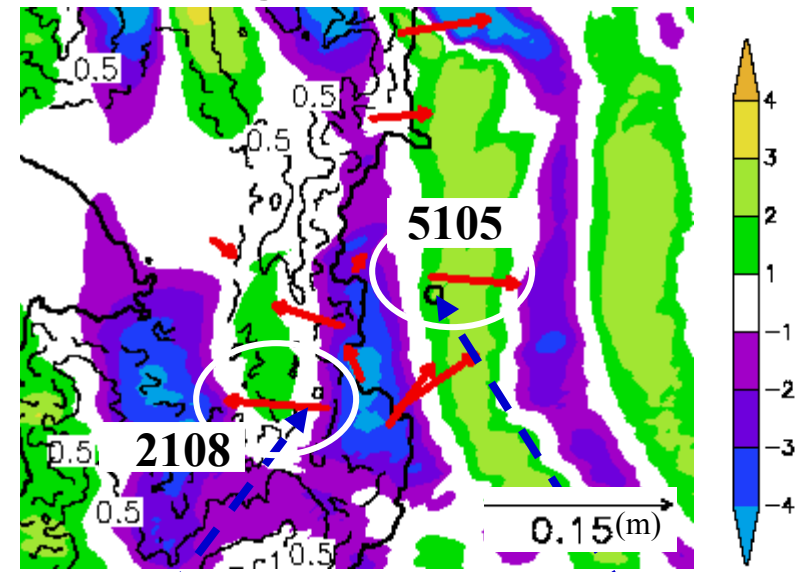
Gradient estimated with 'Linear gradient model'

Linear gradient model: $\tau_{est} = \tau_{zen} m(\theta) + m(\theta) / \tan(\theta) (G_N \cos\phi + G_E \sin\phi)$.

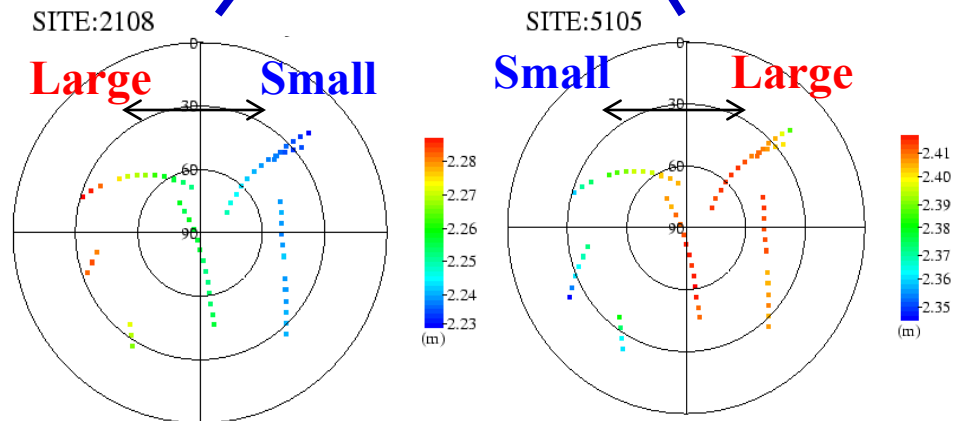
Observed gradient at el.=10°



Simulated gradient at el.=10°



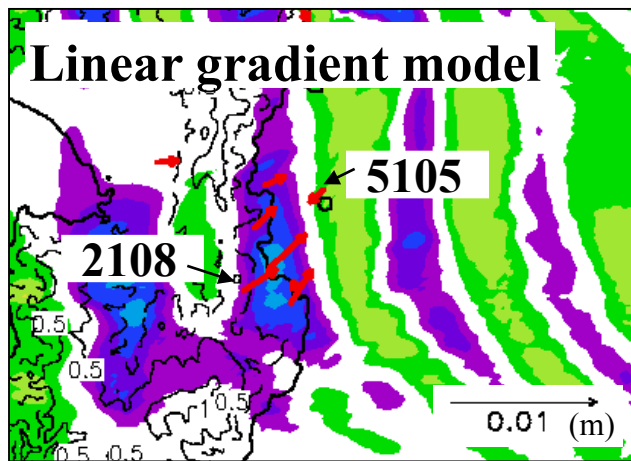
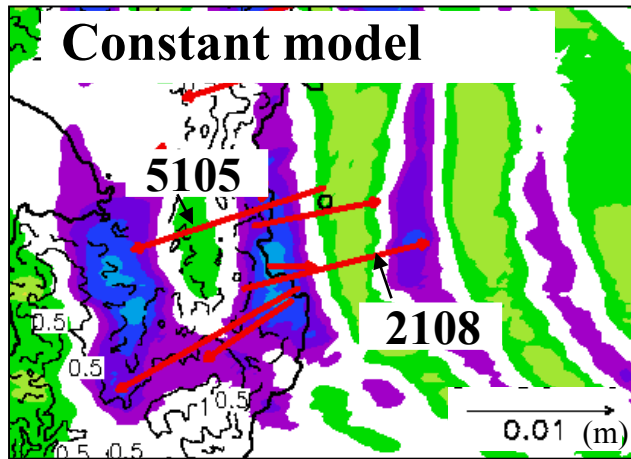
- Simulated gradients pointed to large PWV region from small PWV region.
- Simulated directions of gradient are consistent with observed ones, except KWN and 3042.



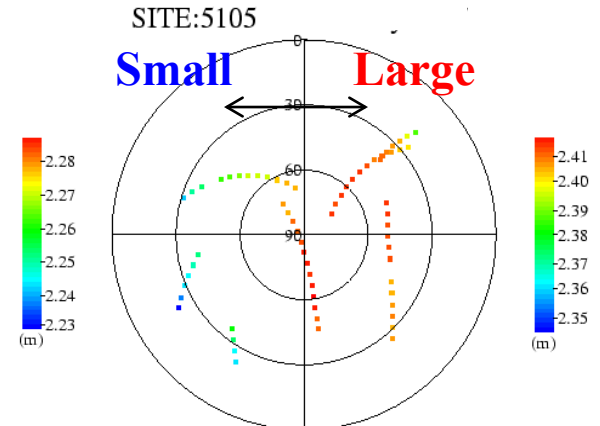
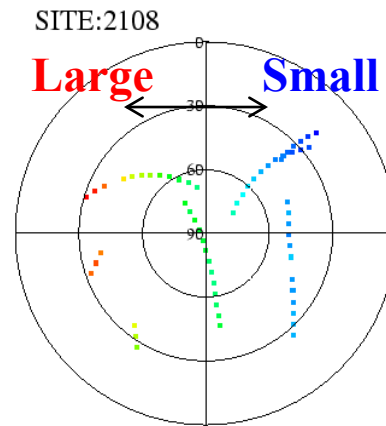
Total delay converted in the zenith direction (m)

Improvement of positioning error by using the gradient

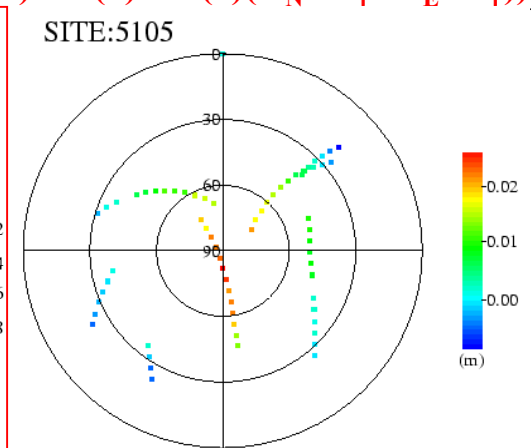
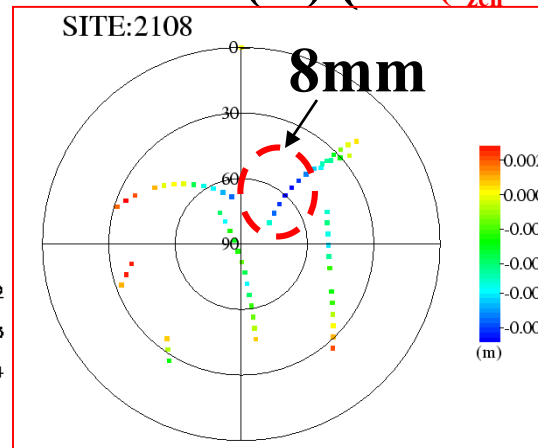
positioning error



Delays in the zenith direction (m)



Residual (m) ($=\tau - (\tau_{zen}m(\theta) + m(\theta)/\tan(\theta)(G_N\cos\phi + G_E\sin\phi))$)



- Positioning error was reduced by using 'Linear gradient model'.
- Large positioning error remained at 2108 where delay did not vary linearly. ← Large residual in red circle causes the large error.

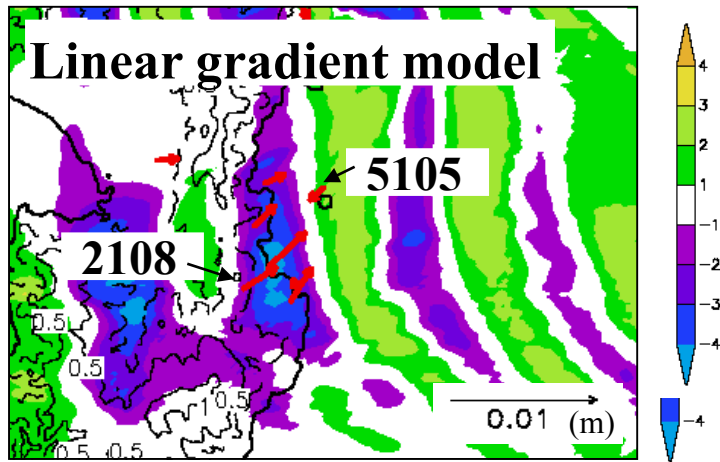
Number of wave in Skymap is a half at most

→ Atmospheric Model is extended to 'Second-order model'

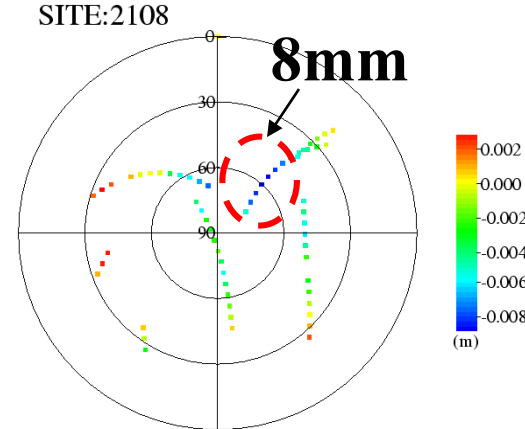
$$\tau_{\text{est}} = \tau_{\text{zen}} m(\theta) + m(\theta)(G_{\text{N}}y + G_{\text{E}}x + G_{\text{N}2}y^2 + G_{\text{NE}}xy + G_{\text{E}2}x^2),$$

where $x = 1.0/\tan(\theta) * \sin\phi$, $y = 1.0/\tan(\theta) * \cos\phi$

positioning error



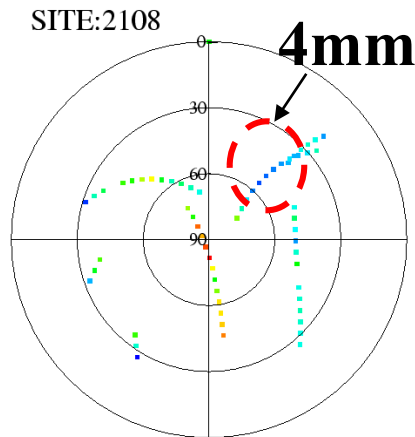
Residual (m) ($=\tau - (\tau_{\text{zen}}m(\theta) + m(\theta)/\tan(\theta)(G_{\text{N}}\cos\phi + G_{\text{E}}\sin\phi))$)



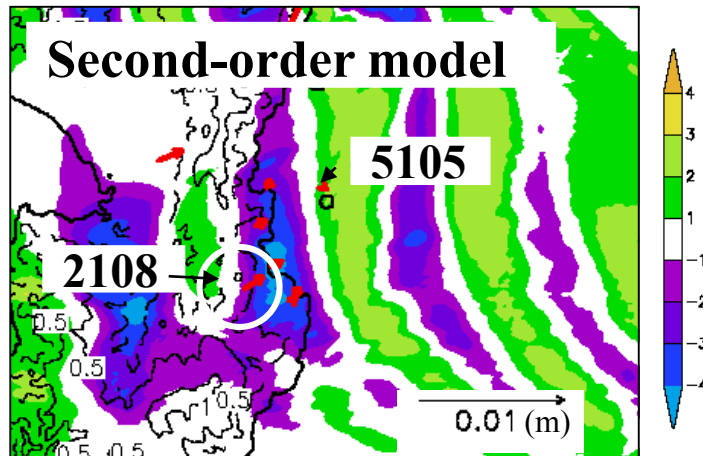
- Large positioning error remained where delay did not vary uniformly (red circle).

Residual (m)

$$(\tau - \tau_{\text{zen}}m(\theta) + m(\theta)(G_{\text{N}}y + G_{\text{E}}x + G_{\text{N}2}y^2 + G_{\text{NE}}xy + G_{\text{E}2}x^2))$$



- Second-order model reduces positioning error.
- Residual in a red circle was decreased.



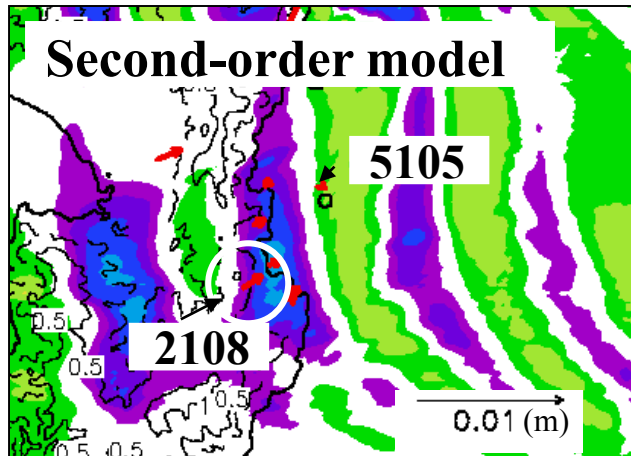
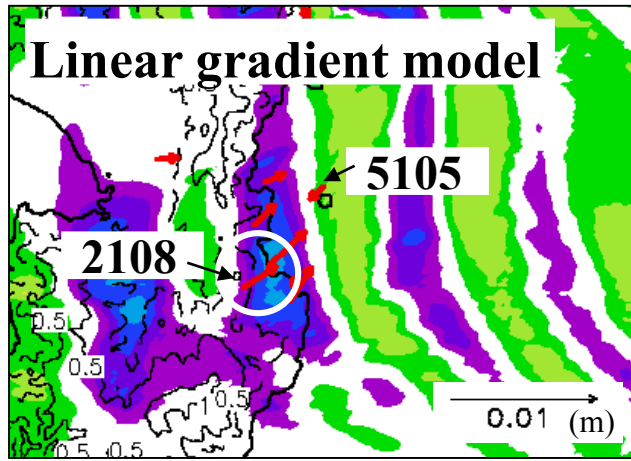
Number of wave in Skymap is a half at most

→ Atmospheric Model is extended to Second-order model

$$\tau_{\text{est}} = \tau_{\text{zen}} m(\theta) + m(\theta)(G_{\text{N}y} + G_{\text{E}x} + G_{\text{N}2}y^2 + G_{\text{NE}xy} + G_{\text{E}2}x^2),$$

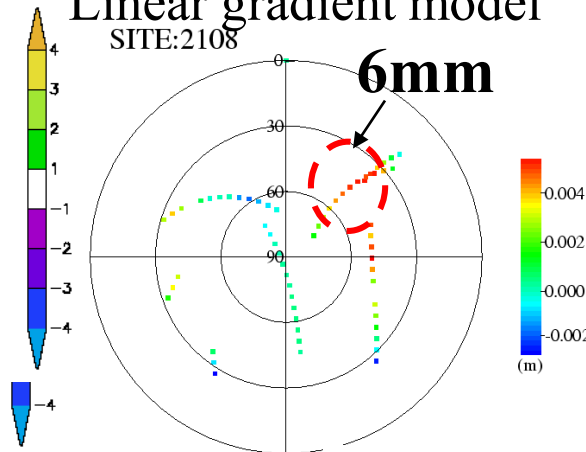
where $x = 1.0/\tan(\theta) * \sin\phi$, $y = 1.0/\tan(\theta) * \cos\phi$

Positioning error

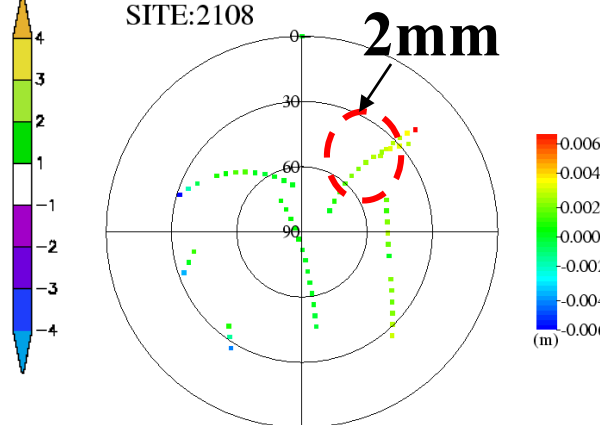


Positioning error in east-west direction (m)

Linear gradient model



Second-order model



- E-W component of residual (O-C) is expressed as $-(\tau - \tau_{\text{est}})\cos\theta\sin\phi$.
- Second order model reduces E-W component of residual (O-C)
- Large residual in a red circle was decreased.

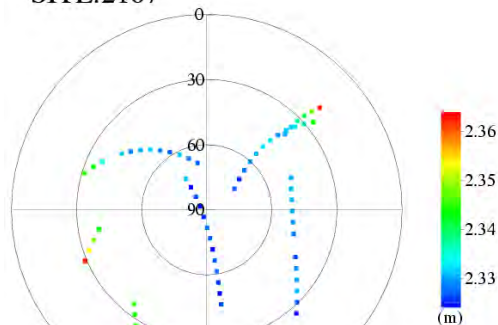
Improvement of vertical positioning error at 2107

$\delta z : -\Sigma\{(\tau - \tau_{est})\sin\theta\}/N$
with linear gradient model

$\delta z : -\Sigma\{(\tau - \tau_{est})\sin\theta\}/N$
with second-order model

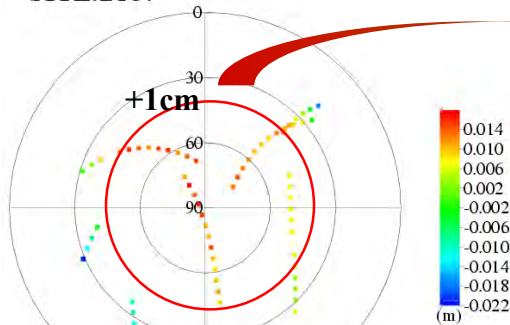
Zenith total delay

SITE:2107



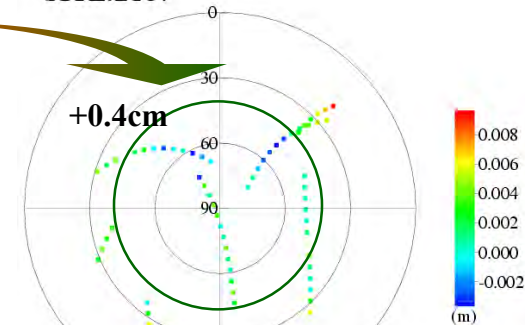
$\delta z = 0.687\text{cm}$

SITE:2107

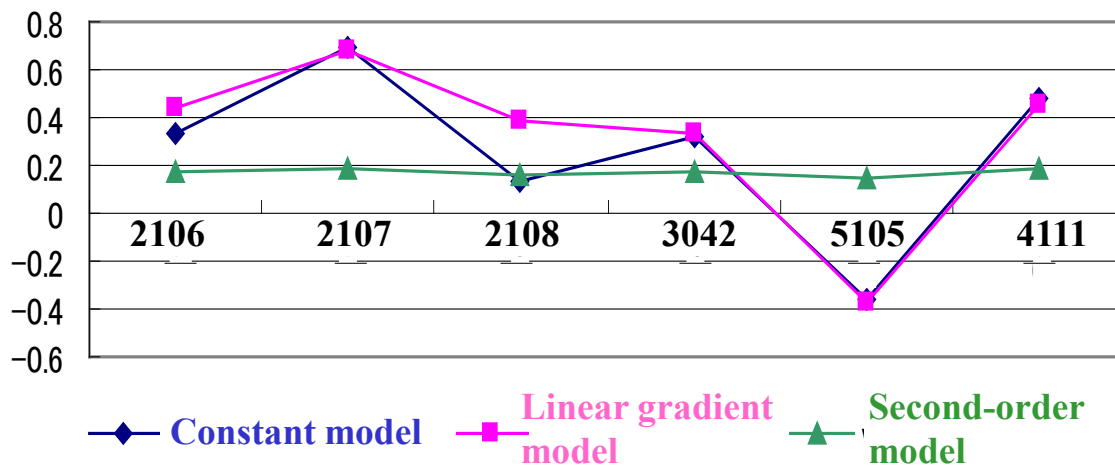


$\delta z = 0.679\text{cm}$

SITE:2107

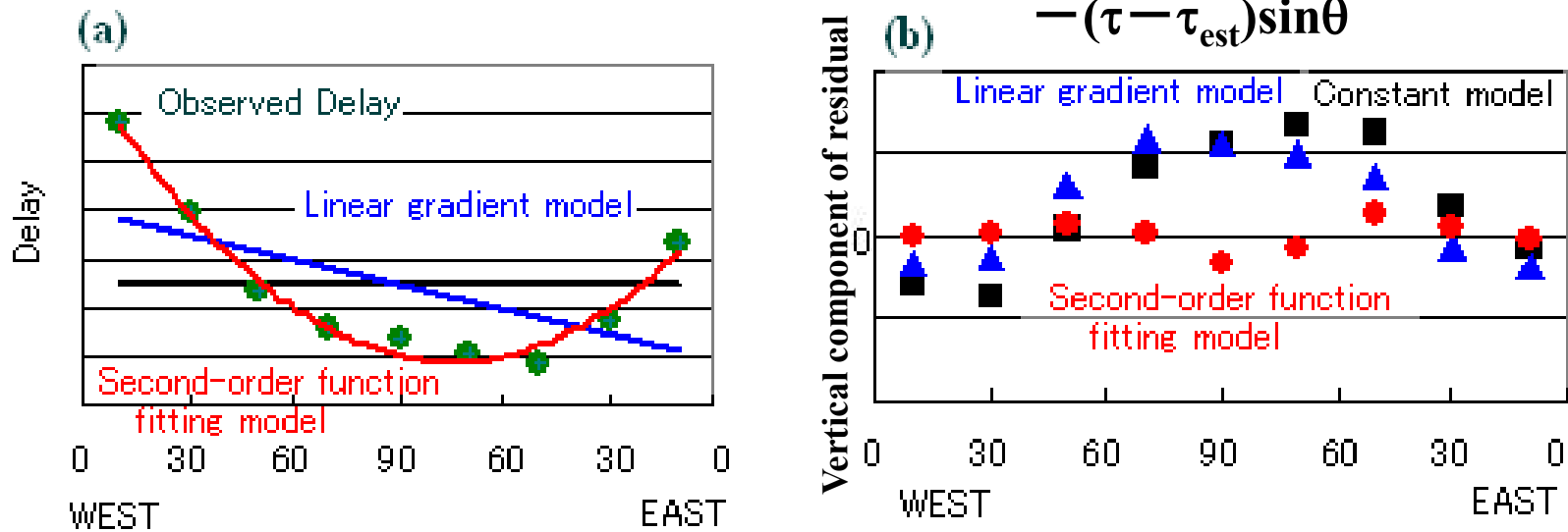


$\delta z = 0.187\text{cm}$



▪ When the delays is estimated with second order model, vertical positioning errors were reduced.

Improvement of vertical positioning error



• 'Constant model', 'Linear gradient model':

Large residual O-C existed at the large elevation angles.

▪ **Vertical component : Large residual was multiplied by $\sin\theta$,**
 \Rightarrow Large vertical positioning error remained.

• 'Second-order function fitting model' :

Residual at the large elevation angle is small

\Rightarrow Vertical positioning error was reduced

5. Summary

- **The positioning error was evaluated with the delays simulated by the numerical weather model.**
Simulated refractivity distributions are useful for evaluation of positioning error.
- **Small scale variation of delay**
 - **Positioning error is greatly reduced by using gradient model.**
 - **Second order curve fitting model improves the positioning error further.**
 - **Second order term is essential for the improvements of vertical positioning error.**

Acknowledgement

This study is the results of the GPS meteorology / Japan. Authors thank Prof. Heki and Dr. Iwabuchi for advising estimation method of the positioning error.